

Crowds reaching targets by maximizing entropy: a Clausius-Duhem inequality approach[★]

Joep Evers^{*} Adrian Muntean^{**} Fons van de Ven^{***}

^{*} ICMS & CASA, Eindhoven University of Technology, P.O. Box 513, 5600 MB Eindhoven, The Netherlands (e-mail: j.h.m.evers@tue.nl).

^{**} ICMS & CASA, Eindhoven University of Technology, P.O. Box 513, 5600 MB Eindhoven, The Netherlands (e-mail: a.muntean@tue.nl)

^{***} CASA, Eindhoven University of Technology, P.O. Box 513, 5600 MB Eindhoven, The Netherlands (e-mail: a.a.f.v.d.ven@tue.nl)

Abstract: In this paper we make a connection between the study of crowd dynamics and concepts from thermodynamics. The basic component of our continuous model is the continuity equation for the density of people, which we complete by prescribing the velocity field. This velocity field includes a nonlocal term modelling interactions between individuals. To provide support for our modelling assumptions we wish to prove an inequality that resembles the Second Law of Thermodynamics. To this end we define an entropy-like functional and show that its time derivative equals a positive dissipation term minus a corrector term. The latter term should be small for the time derivative of the entropy to be positive. In case of isotropic interactions the corrector term is absent. For the anisotropic case we support the claim that the corrector term is small by performing simulations for the corresponding particle system. In fact, this term is sufficiently small for the entropy still to increase. Moreover, we can show that the entropy converges in time towards a limit value.

Keywords: Crowd dynamics, Walking, View angles, Thermodynamics, Entropy, Steady states, First-order systems.

1. INTRODUCTION

Studying the behaviour of people in a crowd is nowadays no longer simply an activity of psychologists and social scientists. During the last few decades, it became clear that understanding and predicting the dynamics of people moving around is extremely important when designing buildings and infrastructure, and when being responsible for the safety of visitors at a large-scale event.

Physicists and mathematicians were the ones who started providing answers to the questions that were posed. Their approach was (and is) similar to the way in which they deal with the physical, non-living world around us. Inevitably, this yields models in which people are nearly treated as if they were non-living material obeying physical laws. Illustrative for this way of thinking is the *social force model*, see e.g. Helbing and Molnár (1995). We remark that more or less in parallel and in the same spirit, the study of vehicular traffic and of biological aggregations (e.g. animal groups) developed.

The difficulty in these models is to determine what the constitutive relations are. In physics, the intuition for these would be provided by experiments. We do not want to

claim that doing experiments with pedestrians is impossible, but in any case it is difficult. One of the issues is the reproducibility.

In this paper we explore a different way of justifying our modelling assumptions. We are interested in showing that a crowd obeys an inequality like the Second Law of Thermodynamics (also called Clausius-Duhem inequality) and thus maximizes ‘entropy’. If we succeed, then this increases the consistency and trustworthiness of our model. For more background on thermodynamic concepts and their context, the reader is referred e.g. to Müller and Ruggeri (1998). Maximizing entropy sounds nearly as if individuals try to win a game or maximize profit. See also Hoogendoorn and Bovy (2003) in this respect.

We first describe our first-order continuum model (Section 2), in particular addressing the constitutive relation we provide to close the model. This is the definition of the velocity field. Next, we introduce in Section 3 a concept of (generalized) entropy. If all interactions are isotropic with respect to the direction in which another individual is perceived, then one can show theoretically that the time derivative of the entropy is positive (in fact, non-negative). More work is required in the anisotropic case. Our numerical illustration in Section 4 suggests however that even in that case the entropy inequality holds. This is

[★] JE kindly acknowledges the financial support of the Netherlands Organisation for Scientific Research (NWO), Graduate Programme 2010.

the main conclusion drawn here. We close the paper with an outlook on future work.

2. MODEL EQUATIONS

Consider the continuity equation

$$\frac{\partial \rho}{\partial t} + \nabla \cdot (\rho v) = 0 \quad (1)$$

on $\mathbb{R}^d \times \mathbb{R}^+$ ($d \in \mathbb{N}^+$ fixed). The model we use is very much in the spirit of Cristiani et al. (2011), be it that their model is formulated in a more general way. Note that we have a *first-order* model, since we prescribe our velocity directly; see Coscia and Canavesio (2008) for an exposition of first-order models *versus* second-order models. We assume that the velocity field is the sum of two contributions

$$v := v_d + v_s, \quad (2)$$

a *desired* velocity v_d , and a *social* velocity v_s . The desired velocity is taken to be a constant, while

$$v_s(x) := \int_{\mathbb{R}^d} g\left(\frac{x-y}{|x-y|} \cdot \frac{v_d}{|v_d|}\right) \nabla W(|x-y|) \rho(y) dy. \quad (3)$$

The term v_s models the interactions between individuals. Note that we often omit the explicit time dependence of our variables. Here, $W : \mathbb{R}^+ \rightarrow \mathbb{R}$ is the potential governing the interactions. We use the word ‘potential’ here, since first-order models can be viewed as overdamped limits of second-order models. In the latter, the ∇W corresponds to a (generalized) force. As such, W is a potential. We refer to Mogilner et al. (2003), p. 360, for a derivation in terms of a particle system.

Here,

$$\nabla W(|x-y|) := W'(|x-y|) \frac{x-y}{|x-y|}. \quad (4)$$

The function $g : [-1, 1] \rightarrow [0, 1]$ incorporates anisotropy in the model. We have in mind the anisotropy that arises due to the fact that people have front and back sides. It depends on the direction in which one person perceives other people, how much influence they have on his motion. We restrict ourselves to linear functions g ; that is, linear in $\frac{x-y}{|x-y|} \cdot \frac{v_d}{|v_d|}$, which is (-1 times) the cosine of the angle under which point x sees point y . See also Gulikers et al. (2012) for our previous investigations on the effect of g on the dynamics of the underlying particle system.

For the sake of being complete, we mention that the work by Coscia and Canavesio (2008) eventually does not focus on the nonlocal dependence on ρ , like in (3). In the cases they investigate in detail, they only allow for local dependence on ρ and/or $\nabla \rho$.

The choice of this velocity field is an ansatz. A way of trying to justify this modelling assumption, is proving that the model is somehow consistent with ideas from thermodynamics. This will be the main motivation for all (mainly formal) steps in the sequel.

As the continuity equation expresses the concept of conservation of mass, we define the total mass

$$\mathcal{M} := \int_{\mathbb{R}^d} \rho(x) dx. \quad (5)$$

Moreover, we define the centre of mass

$$x_0 := \frac{1}{\mathcal{M}} \int_{\mathbb{R}^d} x \rho(x) dx, \quad (6)$$

and the velocity of the centre of mass (or: *barycentric velocity*)

$$v_0 := \frac{dx_0}{dt} = \frac{1}{\mathcal{M}} \int_{\mathbb{R}^d} v(x) \rho(x) dx. \quad (7)$$

Finally, we define the velocity with respect to the velocity of the centre of mass

$$\hat{v}(x) := v(x) - v_0. \quad (8)$$

3. CLAUSIUS-DUHEM-LIKE INEQUALITY

For deriving an entropy-like functional (and corresponding Clausius-Duhem-like inequality) we first define and investigate the following dissipation function $D : [0, T] \rightarrow \mathbb{R}^+$

$$D(t) := \int_{\mathbb{R}^d} \rho(x) |\hat{v}(x)|^2 dx. \quad (9)$$

Here, $T > 0$ is some fixed final time. Note that, since v_d is constant, we have that

$$\begin{aligned} v_0 &= \frac{1}{\mathcal{M}} \int_{\mathbb{R}^d} v(z) \rho(z) dz \\ &= v_d \frac{1}{\mathcal{M}} \int_{\mathbb{R}^d} \rho(z) dz + \frac{1}{\mathcal{M}} \int_{\mathbb{R}^d} v_s(z) \rho(z) dz \\ &= v_d + \frac{1}{\mathcal{M}} \int_{\mathbb{R}^d} v_s(z) \rho(z) dz, \end{aligned} \quad (10)$$

so

$$v(x) - v_0 = v_s(x) - \frac{1}{\mathcal{M}} \int_{\mathbb{R}^d} v_s(z) \rho(z) dz. \quad (11)$$

The second term on the right-hand side of (11) is independent of x . For the dissipation, we now have that

$$\begin{aligned} D(t) &= \int_{\mathbb{R}^d} \rho (v - v_0) \cdot \hat{v} dx \\ &= \int_{\mathbb{R}^d} \rho v_s \cdot \hat{v} dx - \frac{1}{\mathcal{M}} \int_{\mathbb{R}^d} v_s \rho dz \cdot \int_{\mathbb{R}^d} \rho \hat{v} dx \\ &= \int_{\mathbb{R}^d} \rho v_s \cdot \hat{v} dx, \end{aligned} \quad (12)$$

since $\int_{\mathbb{R}^d} \rho \hat{v} dx = 0$, which follows from the definition of \hat{v} . For the ease of notation, let us define

$$\tilde{g}(\xi) := g\left(\frac{\xi}{|\xi|} \cdot \frac{v_d}{|v_d|}\right), \quad (13)$$

for all $\xi \in \mathbb{R}^d \setminus \{0\}$. If we take D and replace x by y (and *vice versa*), we obtain

$$\begin{aligned} D(t) &= \int_{\mathbb{R}^d} \rho(x) \left(\int_{\mathbb{R}^d} \tilde{g}(x-y) \nabla W(|x-y|) \rho(y) dy \right) \cdot \hat{v}(x) dx \\ &= \int_{\mathbb{R}^d} \rho(y) \left(\int_{\mathbb{R}^d} \tilde{g}(y-x) \nabla W(|y-x|) \rho(x) dx \right) \cdot \hat{v}(y) dy \\ &= \int_{\mathbb{R}^d} \rho(x) \int_{\mathbb{R}^d} \tilde{g}(y-x) \nabla W(|y-x|) \cdot \hat{v}(y) \rho(y) dy dx, \end{aligned} \quad (14)$$

by changing the order of integration in the last step. We conclude from (4) that

$$\nabla W(|y-x|) = -\nabla W(|x-y|). \quad (15)$$

Thus,

$$D(t) = - \int_{\mathbb{R}^d} \rho(x) \int_{\mathbb{R}^d} \tilde{g}(y-x) \nabla W(|x-y|) \cdot \hat{v}(y) \rho(y) dy dx. \quad (16)$$

A combination of (12) and (16) yields

$$2D(t) = \int_{\mathbb{R}^d} \rho(x) \int_{\mathbb{R}^d} \nabla W(|x-y|) \cdot V(x, y) \rho(y) dy dx, \quad (17)$$

where

$$\begin{aligned} V(x, y) &:= \hat{v}(x) \tilde{g}(x-y) - \hat{v}(y) \tilde{g}(y-x) \\ &= (\hat{v}(x) - \hat{v}(y)) \left[\frac{1}{2} \tilde{g}(x-y) + \frac{1}{2} \tilde{g}(y-x) \right] \\ &\quad + (\hat{v}(x) + \hat{v}(y)) \left[\frac{1}{2} \tilde{g}(x-y) - \frac{1}{2} \tilde{g}(y-x) \right] \\ &=: (\hat{v}(x) - \hat{v}(y)) \tilde{g}_s(x-y) + (\hat{v}(x) + \hat{v}(y)) \tilde{g}_a(x-y). \end{aligned} \quad (18)$$

Here, \tilde{g}_s and \tilde{g}_a are the symmetric and antisymmetric parts of \tilde{g} , respectively. Thus

$$\begin{aligned} 2D(t) &= \int_{\mathbb{R}^d} \rho(x) \int_{\mathbb{R}^d} \nabla W(|x-y|) \cdot (\hat{v}(x) - \hat{v}(y)) \tilde{g}_s(x-y) \rho(y) dy dx \\ &\quad + \int_{\mathbb{R}^d} \rho(x) \int_{\mathbb{R}^d} \nabla W(|x-y|) \cdot (\hat{v}(x) + \hat{v}(y)) \tilde{g}_a(x-y) \rho(y) dy dx \\ &=: s_s(t) + s_a(t). \end{aligned} \quad (19)$$

Inspired by Carrillo and Moll (2009), we define the following (entropy-like) functional

$$S(t) := \frac{1}{2} \int_{\mathbb{R}^d} \rho(x) \int_{\mathbb{R}^d} W(|x-y|) \tilde{g}(x-y) \rho(y) dy dx. \quad (20)$$

As the function g is linear, we can relate S to s_s . We first note that if g is linear, then \tilde{g}_s is constant. Let us call this constant α .

Lemma 1. If the function g is linear, then

$$\begin{aligned} \frac{dS}{dt} &= \frac{\alpha}{2} \int_{\mathbb{R}^d} \rho(x) \int_{\mathbb{R}^d} \nabla W(|x-y|) \cdot (\hat{v}(x) - \hat{v}(y)) \rho(y) dy dx. \end{aligned} \quad (21)$$

Proof.

$$\begin{aligned} \frac{dS}{dt} &= \frac{1}{2} \int_{\mathbb{R}^d} \frac{\partial \rho(x)}{\partial t} \int_{\mathbb{R}^d} W(|x-y|) \tilde{g}(x-y) \rho(y) dy dx \\ &\quad + \frac{1}{2} \int_{\mathbb{R}^d} \rho(x) \int_{\mathbb{R}^d} W(|x-y|) \tilde{g}(x-y) \frac{\partial \rho(y)}{\partial t} dy dx. \end{aligned} \quad (22)$$

Interchange the order of integration in the first term, and replace x by y (and *vice versa*) in the second term. Since $W(|y-x|) = W(|x-y|)$, we obtain

$$\begin{aligned} \frac{dS}{dt} &= \frac{1}{2} \int_{\mathbb{R}^d} \rho(y) \int_{\mathbb{R}^d} W(|x-y|) \tilde{g}(x-y) \frac{\partial \rho(x)}{\partial t} dx dy \\ &\quad + \frac{1}{2} \int_{\mathbb{R}^d} \rho(y) \int_{\mathbb{R}^d} W(|x-y|) \tilde{g}(y-x) \frac{\partial \rho(x)}{\partial t} dx dy \\ &= \int_{\mathbb{R}^d} \rho(y) \int_{\mathbb{R}^d} W(|x-y|) \tilde{g}_s(x-y) \frac{\partial \rho(x)}{\partial t} dx dy \\ &= -\alpha \int_{\mathbb{R}^d} \rho(y) \int_{\mathbb{R}^d} W(|x-y|) \nabla \cdot (\rho(x) v(x)) dx dy, \end{aligned} \quad (23)$$

where, in the last step, we used the continuity equation and $\tilde{g}_s \equiv \alpha$. Now, apply integration by parts in the x variable (where we assume vanishing boundary terms) to obtain

$$\begin{aligned} \frac{dS}{dt} &= \alpha \int_{\mathbb{R}^d} \rho(y) \int_{\mathbb{R}^d} \nabla W(|x-y|) \cdot v(x) \rho(x) dx dy \\ &= \frac{\alpha}{2} \int_{\mathbb{R}^d} \rho(y) \int_{\mathbb{R}^d} \nabla W(|x-y|) \cdot v(x) \rho(x) dx dy \\ &\quad + \frac{\alpha}{2} \int_{\mathbb{R}^d} \rho(x) \int_{\mathbb{R}^d} \nabla W(|y-x|) \cdot v(y) \rho(y) dy dx \\ &= \frac{\alpha}{2} \int_{\mathbb{R}^d} \rho(x) \int_{\mathbb{R}^d} \nabla W(|x-y|) \cdot v(x) \rho(y) dy dx \\ &\quad - \frac{\alpha}{2} \int_{\mathbb{R}^d} \rho(x) \int_{\mathbb{R}^d} \nabla W(|x-y|) \cdot v(y) \rho(y) dy dx. \end{aligned} \quad (24)$$

In the last step we interchanged the order of integration in the first term, and used (15) in the second term.

All this yields

$$\begin{aligned} \frac{dS}{dt} &= \frac{\alpha}{2} \int_{\mathbb{R}^d} \rho(x) \int_{\mathbb{R}^d} \nabla W(|x-y|) \cdot (v(x) - v(y)) \rho(y) dy dx, \end{aligned} \quad (25)$$

and the desired result then easily follows from the observation that

$$v(x) - v(y) = (\hat{v}(x) + v_0) - (\hat{v}(y) + v_0) = \hat{v}(x) - \hat{v}(y). \quad (26)$$

□

Remark: One can relax the linearity condition on g and obtain the same result. It suffices to have $g'(\eta) = g'(-\eta)$ for all $\eta \in [-1, 1]$. Then $\nabla \tilde{g}_s \equiv 0$ and the corresponding term after integration by parts vanishes. For general (differentiable) g , this term remains, and thus an extra term appears in (21) (and eventually in the entropy inequality we are deriving). These technicalities are however beyond the scope and aim of this paper.

The following equation summarizes our ideas so far in a condensed form:

$$D(t) = \frac{dS(t)}{dt} + s_a(t), \quad (27)$$

or

$$\frac{dS(t)}{dt} = D(t) - s_a(t), \quad (28)$$

which is a more desirable form, as it leads us to an entropy-like inequality. We first observe (by its definition (9)) that $D(t) \geq 0$ for all t . Moreover, we identify the special case $g \equiv 1$, in which we have fully isotropic interactions. To see this, observe in (3) that for $g \equiv 1$ the interaction term in v_s is $\nabla W(|x-y|)$, which is the gradient of a radially symmetric function. Note that in this case $\tilde{g}_s \equiv \tilde{g}$ and

$\tilde{g}_a \equiv 0$. Thus, $s_a(t) = 0$ for all t . As a consequence, we obtain

$$\frac{dS(t)}{dt} = D(t) \geq 0, \quad (29)$$

which is a Clausius-Duhem-type inequality. This is a special case of what was treated by Carrillo and Moll (2009), although there the reduction by subtracting v_0 is not done. If W is bounded, we have an upper bound on S (which is uniform in time). This implies that S will tend to some limiting value as $t \rightarrow \infty$.

Our main question is now whether similar conclusions can be drawn if g is not constant. This is the case in which anisotropy is present in the interactions. In other words, some directions have more influence than others. In general, s_a will no longer be 0. However, if this term is small (compared to D), still

$$\frac{dS(t)}{dt} \geq 0 \quad (30)$$

holds, which is the inequality we are looking for. In the sequel, we test this hypothesis numerically for a specific particle system.

4. NUMERICAL ILLUSTRATION OF THE ANISOTROPIC CASE

For a numerical illustration and investigation of the ideas described before, we simulate the particle system (of size N) corresponding to the model in Section 2. In particular, we take $d = 2$, and choose W to be the *Morse potential*

$$W(s) := C_a e^{-s/l_a} - C_r e^{-s/l_r}, \quad (31)$$

see Mogilner et al. (2003), p. 363, or D’Orsogna et al. (2006) and the references cited therein. Note that D’Orsogna et al. (2006) use this potential in a second-order model. We demand that the parameters are positive and obey $l_r < l_a$ and $C_r/l_r > C_a/l_a$. This makes sure that the interactions are repulsive in the short range, and attractive in the long range. (NB: These conditions include the Case 4 mentioned in Mogilner et al. (2003): $C_r > C_A$ and $l_a > l_r$.)

Furthermore, we take

$$g(\eta) := \frac{1}{2}(1 + \sigma) - \frac{1}{2}(1 - \sigma)\eta. \quad (32)$$

Here $\sigma \in [0, 1]$ is a parameter that is used to tune the amount of anisotropy. If $\sigma = 1$, this corresponds to the isotropic case. Note that σ relates to the aforementioned α via $\alpha = (1 + \sigma)/2$. We test the relatively simple case of $N = 25$, and take only $\sigma = 0.5$ for the sake of brevity. The latter choice ensures that we probe the *anisotropic* case.

Initially the particles (individuals) are distributed randomly over the unit square $[0, 1]^2$. We first show results for one simulation run, and afterwards for a sequence of 1000 runs. New initial conditions are generated in each run.

We want to see whether our numerics comply with $dS/dt \geq 0$. To this end, we show in Fig. 1 the evolution in time of dS/dt . We deduced this quantity in three different ways from our simulations: s_s , the time derivative of S (where S was calculated for the particle system and the numerical time derivative was computed afterwards), and

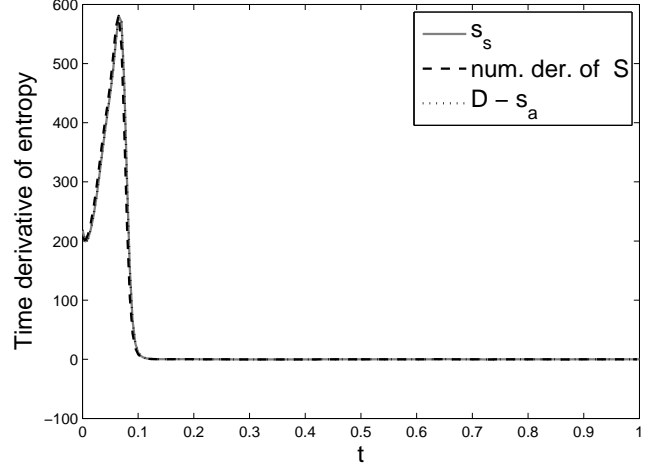


Fig. 1. Plots of s_s , dS/dt (numerical derivative of S), and $D - s_a$ as functions of time. Theory predicts that they should be the same, as is supported by the graphs. It is important to note that the curves are positive and decay to zero (fluctuations around zero are $\mathcal{O}(0.1)$). Results for a single simulation run.

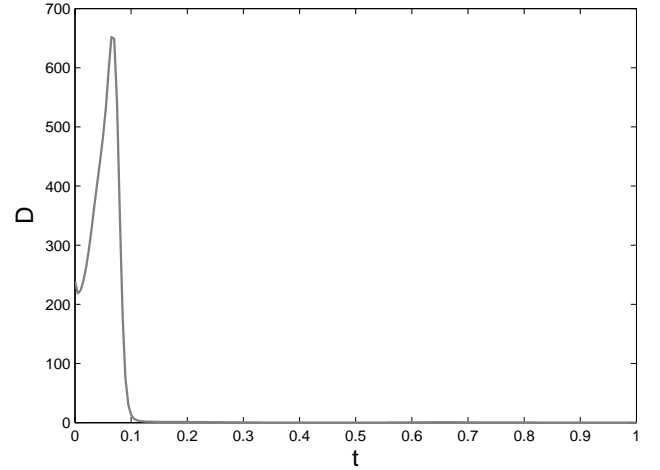


Fig. 2. Plot of D as a function of time. The value decays to zero. Results for a single simulation run.

$D - s_a$. Theoretically these are identical, and the plots show that this is also the case numerically. We will thus not bother about this issue any more in the sequel. The main conclusion we draw from Fig. 1 is that dS/dt is indeed positive and moreover, that it decays to zero.

Next, we examine the behaviour in time of the dissipation D . By definition, D is positive – see (9) – but it turns out that D actually tends to zero as t increases. This is shown in Fig. 2. Note that the behaviour of D is very similar to that of dS/dt .

We observe in Figs. 1 and 2 that there is a sharp transition for $t \approx 0.1$ where the graphs become zero. If $D - s_a$ and D are (nearly) zero, then s_a must also be (nearly) zero. The hypothesis that s_a is small, is thus valid after $t = 0.1$. For the interval $[0, 0.1]$, we investigate the size of s_a separately. In Fig. 3 we show the ratio s_a/D on the interval $[0, 0.1]$. We take this ratio since we are particularly interested in the size of s_a with respect to the size of D . Indeed the values are

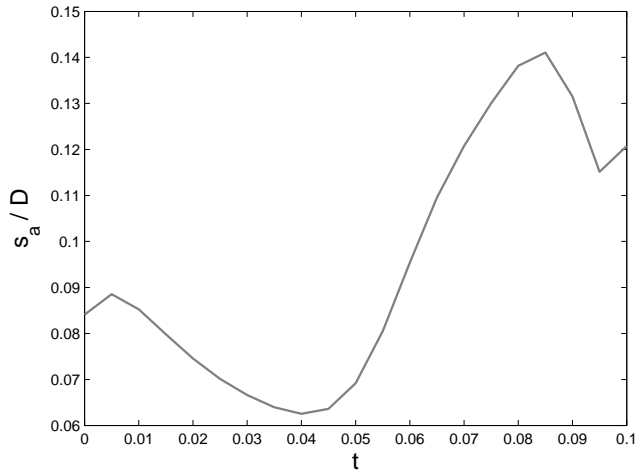


Fig. 3. Plot of s_a/D as a function of time on the interval $[0, 0.1]$. The values are small. Results for a single simulation run.

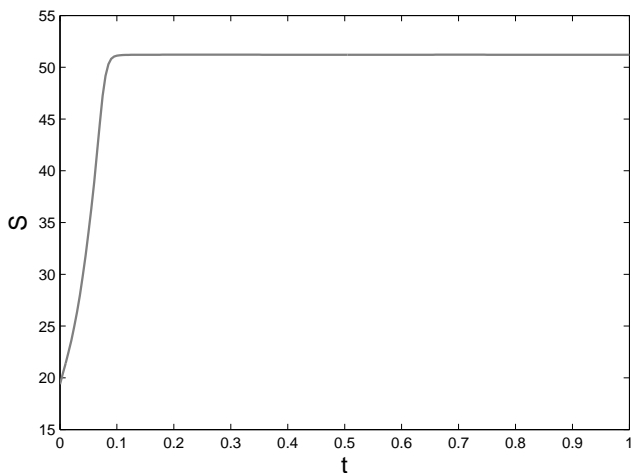


Fig. 4. Plot of S as a function of time. The value approaches a limit value. Results for a single simulation run.

small, i.e. of order $\mathcal{O}(0.1)$. We do not continue the graph after $t = 0.1$ for a simple reason. Since both s_a and D are very small then, we would divide two small numbers to get the ratio s_a/D . The corresponding outcome does not provide any useful information.

The interaction potential W we have taken is bounded. The entropy S therefore has a finite upper bound. As dS/dt is positive (cf. Fig. 1), we expect S to approach a limit value. This is indeed the case, as is shown in Fig. 4.

We check now whether the conclusions we drew from one simulation run also hold if we do multiple runs (where in each run we impose different initial conditions). We do this to be sure that we have not just been ‘lucky’ so far. In Fig. 5 we show two curves corresponding to $D - s_a$. At each time instance, we show both the minimum and maximum over all simulation runs. These graphs provide further evidence that $D - s_a$ (and hence dS/dt) is positive – which follows from the minimum – and decays to zero. Moreover, the term s_a is thus small compared to D . After $t \approx 0.25$ the deviation from zero of the two curves is of order $\mathcal{O}(0.1)$.

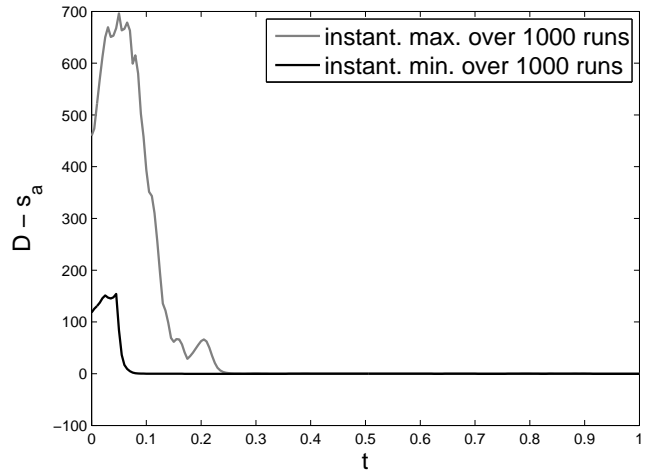


Fig. 5. Plot of $D - s_a$ as a function of time. At every time instance both the maximum and the minimum are taken over 1000 simulation runs. The graphs support the claim that $D - s_a$ is positive and decays to zero.

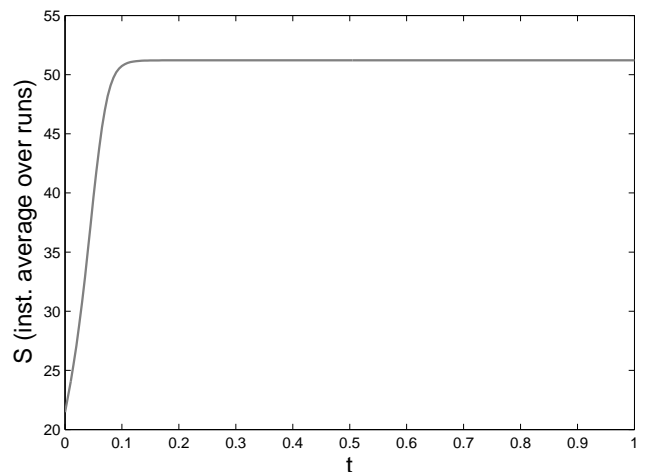


Fig. 6. Plot of S as a function of time. The value approaches a limit value. At every time instance the average is taken over 1000 simulation runs. We checked that in all runs the same limit value was attained.

Taking into account Fig. 5, which shows $dS/dt \geq 0$, we also expect S to increase and eventually converge to a limit. In Fig. 6 we show the average of S over the 1000 runs, and we see that the average indeed increases towards a limit. A plot of $\max_k |S_1(t) - S_k(t)|$ against time (where the index k runs over all simulation instances, and S_1 is hence S obtained from the first simulation run), decays to zero. From this it follows that the limit value is the same in each simulation run. The graph is omitted here.

5. CONCLUSIONS AND OUTLOOK

We start this concluding section by answering the question: What does it actually mean for our system if the dissipation D goes to zero? By the definition of D in (9), $D = 0$ automatically implies that $\hat{v} \equiv 0$. This means that all material points have the same velocity (namely the velocity of the centre of mass $v_0(t)$). For the continuum model, this means that the density profile ρ does not change shape any more; one can show that ρ is con-

served along characteristics $x(t)$ defined by the equation $dx(t)/dt = v_0(t)$. The configuration of the system is then just convected. One should realize however that this does *not* mean that the density ρ is uniform.

By using the definition of S in (20), one can show that it automatically follows from $D \equiv 0$ that S is constant in time.

We remark that the above explanation relates our entropy also to the theory of Lyapunov functionals.

The numerics presented in this paper suggest that even in the case of anisotropic interactions, the dynamics still obey a Clausius-Duhem-type inequality. This supports the idea that it is worthwhile to do more effort to prove this analytically. We are aware of the fact that this fact might only be true under certain technical conditions, which were satisfied (more or less ‘by accident’) in our numerics. One of the aims of further theoretical investigations is to identify these conditions, and make them as sharp as possible. Whereas the isotropic case is nearly a trivial exercise, it is clear from our (unsuccessful) attempts up to now that it will not be an easy task to prove the inequality in the anisotropic case.

We stress here that proving an entropy inequality is not a goal in itself. It provides support for the ‘thermodynamic consistency’ of our model, and as such tells us that our ansatz for the velocity field is admissible, and hence, our modelling is not completely wrong.

To get a better understanding of what exactly to prove, and how to proceed towards these proofs, we suggest to do first some more numerical experiments. In particular, we would pay attention to the following aspects:

- One can do the same simulations, but change the value of σ . Note that $\tilde{g}_a(x - y)$ is proportional to $(1 - \sigma)$, and this factor thus appears in s_a . The amplitude of this term most likely increases automatically with decreasing σ ($\sigma \downarrow 0$).¹ Following this line of argument, it might be true that dS/dt is only positive for σ within a certain distance from 1. This would lead to a condition on σ ; possibly a condition in which σ is combined with other quantities.
- Increase the number of particles N . One might guess that in a certain scaling, one can obtain the continuum model treated in this paper from the corresponding particle system that was used in the simulation section. The bigger N , the closer we then hope the result to be to the results of the continuum model. In this paper, a relatively small N was used, to have a system of ODEs that can still be handled easily. After all, the numerics in this paper only intend to illustrate our ideas and confirm our conjectures.
- It would be interesting to see whether our results depend on the precise choice of interaction potential W . The simplest way would be to have different parameters (C_r, C_a, l_r, l_a) . However, it is much more interesting to try another type of potential (possibly with a singularity around the origin). If the repulsive

behaviour around the origin is e.g. of the type $\sim 1/r$ (cf. Coulomb interactions), we lose the trivial upper bound on S that followed from $\|W\|_\infty$. Numerics should then provide insight in whether the entropy still increases towards a limit value. Also, one could especially look at potentials that only model a zone of repulsion (that is, no attraction zone). This is interesting, since for repulsive interactions mass will ‘diffuse’ and for each x fixed $\rho(x, t) \rightarrow 0$ as $t \rightarrow \infty$. This implies that no steady states are to be expected. To what extent this destroys our entropy inequality is yet to be investigated.

REFERENCES

- Carrillo, J. and Moll, J. (2009). Numerical simulation of diffusive and aggregation phenomena in nonlinear continuity equations by evolving diffeomorphisms. *SIAM J. Sci. Comput.*, 31, 4305–4329.
- Coscia, V. and Canavesio, C. (2008). First-order macroscopic modelling of human crowd dynamics. *Math. Mod. Meth. Appl. Sci.*, 18(suppl.), 1217–1247.
- Cristiani, E., Piccoli, B., and Tosin, A. (2011). Multiscale modeling of granular flows with application to crowd dynamics. *Multiscale Model. Simul.*, 9(1), 155–182.
- D’Orsogna, M., Chuang, Y., Bertozzi, A., and Chayes, L. (2006). Self-propelled particles with soft-core interactions: Patterns, stability, and collapse. *Phys. Rev. Lett.*, 96, 104302.
- Gulikers, L., Evers, J., Muntean, A., and Lyulin, A. (2012). The effect of perception anisotropy on particle systems describing pedestrian flows in corridors. CASA Report No. 12-36, Eindhoven University of Technology. See also arXiv:1210.4530.
- Helbing, D. and Molnár, P. (1995). Social force model for pedestrian dynamics. *Phys. Rev. E*, 51(5), 4282–4286.
- Hoogendoorn, S. and Bovy, P. (2003). Simulation of pedestrian flows by optimal control and differential games. *Optim. Control Appl. Meth.*, 24, 153–172.
- Mogilner, A., Edelstein-Keshet, L., Bent, L., and Spiros, A. (2003). Mutual interactions, potentials, and individual distance in a social aggregation. *J. Math. Biol.*, 47, 353–389.
- Müller, I. and Ruggeri, T. (1998). *Rational Extended Thermodynamics*. Springer Verlag.

¹ One should however be careful here in drawing this conclusion. Taking σ closer to 0 also changes the dynamics which, in turn, might cause a change in the integral term over ρ in s_a . This change could possibly counterbalance the change in $1 - \sigma$ in such a way that our claim on the size of s_a does not hold.